Macromolecules

Article

pubs.acs.org/Macromolecules

Diyne-Functionalized Fullerene Self-Assembly for Thin Film Solid-State Polymerization

Jean-Nicolas Tisserant,[†,§] Roland Hany,[†] Eric Wimmer,[†] Antoni Sánchez-Ferrer,[§] Jozef Adamcik,[§] Gaëtan Wicht,[†] Frank Nüesch,[†,∥] Daniel Rentsch,[†] Andreas Borgschulte,[‡] Raffaele Mezzenga,[§] and Jakob Heier*[,†]

[†]Swiss Federal Laboratories for Materials Science and Technology, Laboratory for Functional Polymers, Empa, Überlandstrasse 129, CH-8600 Dübendorf, Switzerland

[‡]Swiss Federal Laboratories for Materials Science and Technology, Laboratory for Hydrogen and Energy, Empa, Überlandstrasse 129, CH-8600 Dübendorf, Switzerland

[§]Department of Health Sciences and Technology, Institute of Food, Nutrition and Health, ETH Zürich, CH-8092 Zürich, Switzerland

[∥]Institut des Matériaux, Ecole Polytechnique Fédérale de Lausanne, EPFL Station 12, CH-1015 Lausanne, Switzerland

Supporting Information

ABSTRACT: C_{60} fullerene derivatives bearing aliphatic chains can self-assemble into versatile supramolecular structures. Cross-linking of such self-assembled morphologies is an attractive approach to enhance the structural stability of these self-organized structures. We describe the synthesis of a C_{60} functionalized with a single alkyl chain bearing a diacetylene moiety. In a thin film, the molecule self-assembles into lamellar arrays. The character of the side chain attached to the fullerene is key to the observed packing ability. The stabilization proceeds through solid-state polymerization of the diacetylene moieties. By blending the fullerene derivative with a cyanine dye, various nanostructured fullerene morphologies are obtained that can be selectively stabilized by thermal polymerization. These films can serve as basis for nanostructured fullerene scaffolds that can find applications in optics and electronics.

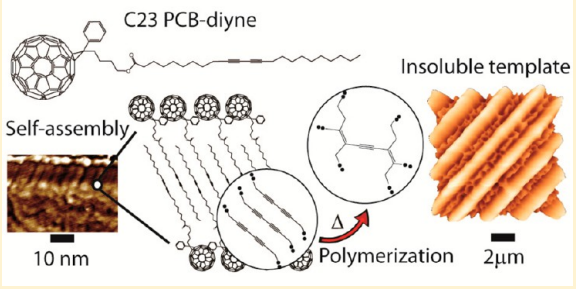

INTRODUCTION

Organic semiconducting molecules in thin films offer promising alternatives to inorganic semiconductors in the fields of both electronics and optics. Besides numerous other appealing characteristics, fullerenes have attracted attention as they belong to the class of small molecule n-type organic semiconductors with excellent electronic properties.[1,2] Fullerenes and their derivates have been shown to self-assemble into various mesoscopic shapes that can be controlled by the chemical nature of their side group.[3−6] A well-known route for molecular self-assembly is based on amphiphilic molecules. For instance, amphiphilic fullerenes containing cations[7] or anions[8] associate into bilayers that assemble into nanorods or vesicles. A lot of attention has been paid to structures formed from alkylated fullerenes. The nature of these molecules is not strictly hydrophobic−hydrophilic, but it rather shows a "hydrophobic amphiphilicity" due to $\pi-\pi$ interacting C_{60} and the van der Waals interacting alkyl chain.[9,10] Nakanishi et al. synthesized a fullerene derivative with three hexadecyl chains. From a bilayer composed of C_{60} and interdigitated alkyl chains, fibers, disks, spheres, and cones form, depending on the solvent.[11] The same system assembled epitaxially on highly oriented pyrolytic graphite (HOPG), forming lamellar structures resulting in a 1D alignment of the fullerenes.[12] Self-organized structures as described above have proven to be a very efficient way to facilitate solid-state polymerization, which stabilizes a morphology without destroying it. Wang et al. incorporated diacetylene functional groups into a fullerene derivative known to self-assemble into a bilayer structure on the molecular level.[10] The cross-linked material was remarkably resistive against organic solvents. For fullerene derivatives several cross-linking routes have been explored, including epoxydes,[13] styrene derivatives,[14] oxetanes,[15] or polyacetylenes.[16,17]

Polymerization of diacetylenes proceeds through a 1,4 topochemical cycloaddition which Werner first described in 1969 as a diffusion-free, entirely lattice-controlled process.[18] Schmidt later proposed a mechanism for such a solid-state reaction based on 2 + 2 cycloaddition of olefins.[19] Topochemical reactions retain position and symmetry of the monomer units; they require a stacked arrangement of monomer units such that one unit can react with its two neighbors.[20−22] Conjugated diacetylenes polymerize in the

Received: August 9, 2013
Revised: December 20, 2013
Published: January 13, 2014

solid state under the influence of pressure, heat, UV, or γ radiation to yield conjugated structures.[23]

Phase separation and dewetting are well-established methods to manufacture nanostructured thin films with new functionalities. Cross-linking would be most attractive if applied to the phase of a blend film such that insoluble meso- or macroporous structured scaffolds can be manufactured.[24] Fullerene blend films with various electron donors are currently widely studied for organic solar cell applications.[25] Most studied are blends with semiconducting polymers,[26−28] but blends with small organic molecules have gained great interest.[29] Stabilizing specific blend morphologies of fullerenes is appealing as it is believed that coarsening of the nanomorphology impacts device performance.[13] In our previous work, we have shown that liquid−liquid dewetting (LLD) is the dominant phase-separation process in blends of polymers and cyanine dyes, providing easy means of hierarchical structuring.[30]

Microcontact printing (μCP) of functional thiols on surfaces[31,32] is a well-described method to induce long-range order in a dewetting[33] or phase-separating[34] system. We have shown in a previous study that the pattern replication could be controlled by the contact line pinning of hydrophobic droplets of phenyl-C_{61}-butyric acid methyl ester (PCBM) on hydrophobic self-assembled monolayer (SAM) lines.[35] The ability to stabilize such fullerene patterns and meso-structures is a new concept and may prove useful for further processing of these functional surfaces. We here demonstrate the synthesis of a C_{60} derivative carrying an alkyl chain with one single diyne moiety to (i) enhance the self-assembly of the fullerene and (ii) polymerize the mesoscopic structure obtained both in bulk films and microstructured films achieved by a phase separation process.

EXPERIMENTAL SECTION

Synthesis of PCB-Diynes. The synthesis shown here for the first time used only commercially available reactants and mild conditions. Scheme 1 shows the two-step synthesis of the diacetylene-functionalized fullerene derivatives. In a first reaction, PCBM was reduced to the corresponding alcohol PCB-ol using diisobutylaluminium hydride (DIBAL). PCB-ol was then esterified with diynoic acids in the presence of *N*,*N*′-dicyclohexylcarbodiimide (DCC) and 4-(dimethylamino)pyridine (DMAP) to yield C23 and C11 PCB-diyne.

Scheme 1. Synthetic Route for Obtaining PCB-Diyne via Reduction of PCBM with DIBAL and Steglich Esterification with Diynoic Acid[a]

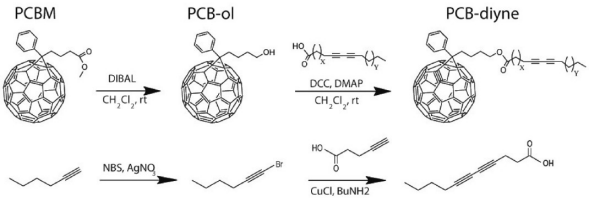

[a]10,12-Tricosadiynoic acid was commercially available; 4,6-undecadiynoic acid was synthesized via coupling of 1-bromohexyne and 4-pentynoic acid.

4-([6,6]-Phenyl-C_{61})butanol, PCB-ol. PCBM (500 mg) was placed in a dry 500 mL round-bottom flask under argon, and then 150 mL of dry CH_2Cl_2 was added and cooled to 0 °C. 5 equiv of DIBAL (1 M in CH_2Cl_2) was added dropwise under stirring. The reaction was run overnight at room temperature. CH_3OH (4 mL) was then added, and the organic layer was washed two times with water. The aqueous layer was then extracted twice with CH_2Cl_2, the organic phase was collected and dried over $MgSO_4$, and the solvent was then removed under reduced pressure. The crude product was dissolved in CH_2Cl_2 and purified by column chromatography (Silica gel 60, Merck as stationary phase, CH_2Cl_2 as eluent). After drying, 420 mg (87% yield) of PCB-ol was obtained.

10,12-Tricosadiynoic Acid [6,6]-Phenyl-C_{61}-butyl Ester, C23 PCB-Diyne. 150 mg of PCB-ol was placed in a dry round-bottom flask under argon atmosphere, and then 125 mL of dry CH_2Cl_2 was added with stirring at room temperature. A mixture of 294 mg of 10,12-tricosadiynoic acid, 262 mg of DCC, and 16 mg of DMAP dissolved in 25 mL of dry CH_2Cl_2 was then added at room temperature in the dark. The solution was stirred in the dark for 4 days. The solvent was removed under reduced pressure, and the crude product was purified by column chromatography (Silica gel 60, Merk as stationary phase, and hexane/CH_2Cl_2, 2:1 as eluent). After that, the solid was washed twice with CH_3OH. After filtration and drying, 160 mg of C23 PCB-diyne was obtained (78% yield). Chemical structures and purities were verified by ^{1}H NMR and mass spectrometry (MS) (see Supporting Information).

Synthesis of C11 Diynoic Acid. *1-Bromo-1-hexyne.* In a three-necked flask, 0.8 g of 1-hexyne, 1.96 g of *N*-bromosuccinimide (NBS), 0.17 g of $AgNO_3$, and 50 mL of acetone were added. The mixture was stirred for 3 h at room temperature, mixed with 100 mL of hexane, and concentrated under reduced pressure. The solid phase was removed by filtration, and the filtrate was purified by fractional distillation under reduced pressure. 740 mg of yellow oil was obtained (45% yield). ^{1}H NMR (400.1 MHz, $CDCl_3$): 2.16 (t, J = 7.0 Hz, 2H), 1.45 (m, 2H), 1.37 (m, 2H), 0.86 (t, J = 7.3 Hz, 3H) ppm.

4,6-Undecadiynoic Acid. In a three-necked flask, 17.8 mg of copper(I) chloride and 20 mL of 30% butylamine aqueous solution were added. A few crystals of hydroxylamine hydrochloride were added to the solution until the blue color disappeared. 300 mg of 4-pentynoic acid was added, and the mixture was cooled to 0 °C. 700 mg of 1-bromo-1-hexyne in 10 mL of diethyl ether was added dropwise. The solution was then stirred at room temperature for 2 h and was stopped with 2 N HCl by adjusting the pH to 2. The organic layer was extracted three times with ethyl acetate. The organic layers were collected and dried, and the solvent was removed under reduced pressure. The crude product was recrystallized in hexane. 390 mg of 4,6-undecadiynoic acid was obtained (71% yield). ^{1}H NMR (400.1 MHz, $CDCl_3$): 2.59 (m, 4H), 2.25 (t, J = 6.9 Hz, 2H), 1.49 (m, 2H), 1.41 (m, 2H), 0.90 (t, J = 7.3 Hz, 3H) ppm.

4,6-Undecadiynoic Acid [6,6]-Phenyl-C_{61}-butyl Ester, C11 PCB-Diyne. C11 PCB-diyne was synthesized by coupling PCB-ol with 4,6-undecadiynoic acid, as described above for C23 PCB-diyne. Yield 20%. ^{1}H NMR (400.1 MHz, $CDCl_3$): 7.92 (m, 2H), 7.55 (m, 2H), 7.48 (m, 1H), 4.18 (t, J = 6.3 Hz, 2H), 2.89 (m, 2H), 2.51 (m, 4H), 2.24 (t, J = 6.9 Hz, 2H) 1.8−2.0 (m, 4H), 1.48 (m, 2H), 1.40 (m, 2H), 0.89 (t, J = 7.2 Hz, 3H) ppm.

General Methods. PCBM (Solenne B.V., The Netherlands) and 10,12-tricosadiynoic acid (Sigma-Aldrich) were used as received; the cyanine dye 1,1′-diethyl-3,3,3′,3′-tetramethylcarbocyanine perchlorate (CyC) was synthesized in our laboratory.[36] Films were spin-coated on glass substrates at different spin speeds (250−4000 rpm) from a 1 wt % solution of PCB-diyne, PCB-diyne/CyC, or PCBM/CyC in chlorobenzene (CB). The composition of blends varied from 0.8:1 to 2:1 (mol/mol) between CyC and the fullerenes. Films were temperature-annealed at 100 or 120 °C in the dark under vacuum (10^{-3} mbar) for times ranging from 1 to 24 h. To check the (in)solubility, films were immersed in a large volume (typically 50 mL for a 1 cm^2 film) of a good solvent (CB, CH_2Cl_2, or $CHCl_3$) and were sonicated for 10 min.

Film characterization included scanning force microscopy (SFM), optical microscopy, UV−vis spectroscopy, attenuated total reflectance Fourier transform infrared (ATR-FTIR) spectroscopy, and Raman spectroscopy. SFM images were measured on a Nanosurf Mobile S in tapping mode at a resonance frequency of 170 kHz with rectangular silicon cantilevers (Mikromasch, Nanosensors TM) with a typical force constant of ~40 N m^{-1} and a tip radius of ~10 nm; images were

dx.doi.org/10.1021/ma401677v | Macromolecules 2014, 47, 721−728

analyzed with the WsXM scanning probe microscopy software.[37] High-resolution SFM images were collected using a Nanoscope 8 multimode scanning force microscope (Bruker) operated in tapping mode under ambient conditions. The microscope was covered with an acoustic hood to minimize vibrational noise. The cantilevers with a nominal tip radius of <10 nm (Bruker) were driven at oscillation frequencies in the range of 150−200 kHz. Images were flattened using the Nanoscope 8.1 software, and no further image processing was carried out. Attenuance spectra taking scattering into account were measured on a Varian Cary 50 UV−vis spectrophotometer. ATR-FTIR spectra were measured on a Bio-Rad FTS 6000 spectrophotometer for powders and a Bruker Hyperion (ATR coupled to an optical microscope) for measurements on thin films. Raman spectra were collected on a Senterra (Bruker) Raman microscope. To avoid long-term exposure to the high intensity of the Raman laser, many short measurements were taken at various positions of the sample. The data was averaged over 50 spectra taken at λ = 532 nm with the lowest possible laser power of 0.2 mW focused on an area of 5 μm^2. Differential scanning calorimetry (DSC) was measured on a PerkinElmer DSC 8000 (under nitrogen flow, at heating/cooling rates of 10 °C min^{-1} from 20 to 140 °C). Thermogravimetric analysis (TGA) experiments were conducted on a Netzsch TG under an argon atmosphere, with a heating rate of 20 °C min^{-1}, from 30 to 900 °C. Wide-angle X-ray scattering (WAXS) experiments were performed using a Rigaku MicroMax-002+ microfocused beam (4 kW, 45 kV, 0.88 mA) with the $\lambda_{Cu\ K\alpha}$ = 0.154 18 nm. The scattering intensities were collected in transmission mode by a Fujifilm BAS-MS 2025 imaging plate system (15.2 × 15.2 cm^2, 50 μm resolution). An effective scattering vector range of 0.5 $nm^{-1} < q < 25\ nm^{-1}$ was obtained, where q is the scattering wave vector defined as $q = 4\pi \sin\theta/\lambda_{Cu\ K\alpha}$ with a scattering angle of 2θ. Samples for WAXS were drop-cast from chlorobenzene solutions (10 g L^{-1}) on freshly cleaved mica substrates (Pelco Mica Discs,Ted Pella, Inc.) and subsequently annealed as described earlier.

Preparation of Patterned Substrates. Metals for thermal deposition were purchased from Cerac Inc. 3 nm of chromium thermally deposited onto glass served as an adhesion layer for the deposition of 10−30 nm of gold. Both metals were deposited at a rate of 0.1 Å s^{-1} and at a starting pressure of 6 × 10^{-6} mbar. The poly(dimethylsiloxane) (PDMS) stamps were prepared by molding a 10:1 (wt) base:curing agent mixture (Sylgard 184-Dow Corning) on a silicon wafer micropatterned by photolithography. After curing at room temperature for 24 h, a drop of 0.5 mM ethanolic solution of octadecanethiol (Sigma-Aldrich) was deposited on the PDMS stamp for 5 s. The stamp was dried under nitrogen for 10 s and held in contact with the gold surface for 10 s. The substrates were washed with ethanol before coating.

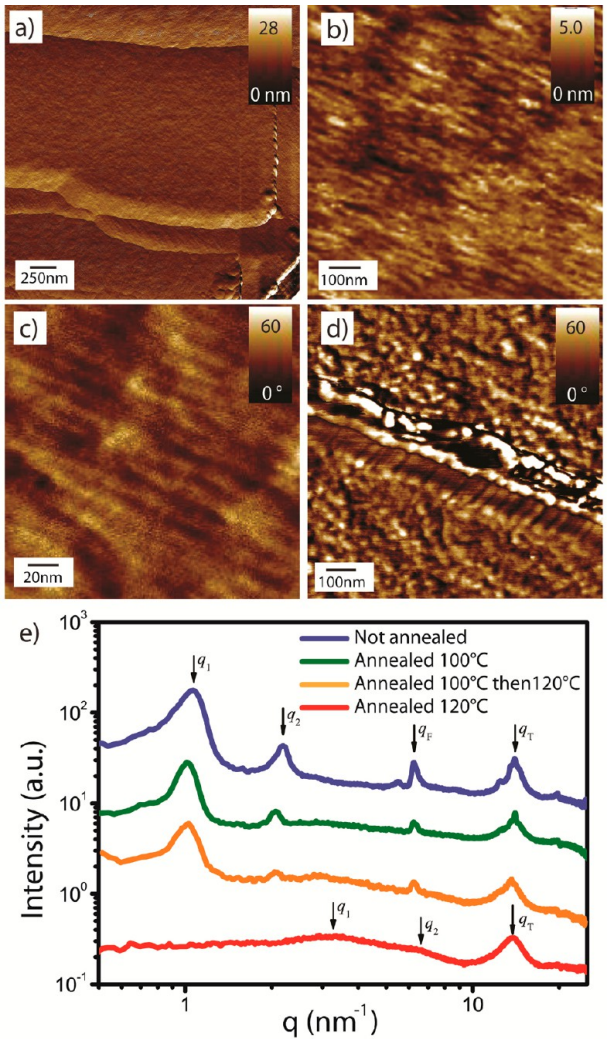

Figure 1. (a) SFM image of a single crystalline platelet drop-cast from 10 mg mL^{-1} C23 PCB-diyne in CB. (b−d) SFM images on such a platelet showing a periodic packing of the monomers with a periodicity of ca. 8 nm. (e) WAXS data measured on a film as cast (blue), on a film annealed for 24 h at 100 °C (green), on a film annealed for 24 h at 100 °C, then for 3h at 120 °C and measured at 120 °C (orange), and for 8 h at 120 °C (red).

RESULTS AND DISCUSSION

Self-Assembly of PCB-Diyne. We first discuss the self-assembly of a C_{60} derivative where the fullerene is linked via an ester to an alkyl chain (C23 or C11) bearing a conjugated diacetylene moiety. The synthesis route for C23 and C11 PCB-diyne is shown in Scheme 1 and described in the Experimental Section. In films obtained by drop-casting of the C23 diyne molecule from CB solution, micrometer-large polycrystalline domains form (Figure 1a). High-resolution scanning force microscopy (SFM) images reveal that the molecules pack in a 1D periodic lattice fashion with a typical periodicity of ca. 8 nm (Figures 1b−d). We can identify regions where the lamellae are oriented perpendicularly to the substrate (Figures 1b,c). A grain boundary between two crystalline plates is shown in Figure 1d. The lamellar packing of the molecules was revealed by wide-angle X-ray scattering (WAXS) experiments as shown in Figure 1e. Two sharp reflections are observed at low q-values at q_1 = 1.06 nm^{-1} and at $q_2 = 2q_1$, which correspond to a lamellar packing of the PCB-diyne molecules with a layer distance of d_1 = 5.92 nm and a correlation length of ξ_1 = 31.4 nm. This lamellar periodicity indeed corresponds to the total length of two interdigitated PCB-diyne molecules (see Figure S7, Supporting Information). At high q-values, a sharp reflection at q_F = 6.28 nm^{-1} and a set of peaks at q_T = 12.4, 13.6, and 14.0 nm^{-1} are visible and correspond to the fullerene−fullerene distance of d_F = 1.00 nm (ξ_F = 20.4 nm) and the crystalline packing of the alkyl tails with an average distance around d_T = 4.5 Å (ξ_T = 51.3 Å), respectively. We therefore suggest that the lamellae shell is composed of C_{60}, while the alkyl chains are interdigitated and aligned with a periodicity of 0.45 nm. The difference between the periodicity observed is WAXS and SFM may arise from surface tilting. Some SFM scans suggest a hexagonal packing of cylinders (see Figure S8, Supporting Information); this morphology is not supported by WAXS and could be assigned to a surface layer which forms in film regions where lamellae are oriented parallel to the substrate, but the thickness is irreconcilable with the lamellar period. Upon thermal annealing of such films, WAXS data reveal that two

dx.doi.org/10.1021/ma401677v | Macromolecules 2014, 47, 721−728

different morphologies develop depending on the annealing temperature during the polymerization process. Annealing the sample at 100 °C keeps the lamellar structure of the samples and the crystallinity of the alkyl domains as observed by the two sharp reflections at q_1 = 1.02 nm^{-1} and q_2 = 2.06 nm^{-1} and the set of peaks at q_T = 12.4, 13.6, and 14.1 nm^{-1}, respectively. The corresponding distances to these two features are the layer distance d_1 = 6.18 nm with a correlation length of ξ_1 = 38.3 nm and the average distance between alkyl tails of d_T = 4.5 Å (ξ_T = 48.6 Å). Moreover, a sharp peak at q_F = 6.28 nm^{-1} is also present which indicates that the fullerene moieties are well packed into their domain with an interfullerene distance of d_F = 1.00 nm (ξ_F = 19.4 nm). Temperature-dependent WAXS experiments revealed that this lamellar structure is stable against further annealing at 120 °C, and only the alkyl chains melt, which is shown by a broadening of the peak at q_T while the peaks at q_1, q_2, and q_F are maintained. This morphological stability will be discussed further when considering the topochemical polymerization of C23-PCB-diyne. Annealing the sample directly at 120 °C induces a transition to the amorphous state as observed by the presence of a single broad peak at q_T = 13.7 nm^{-1} which corresponds to the tail-to-tail distance of d_T = 4.6 Å. Moreover, the fullerene moieties are dispersed into the polymerized alkyl tail matrix as shown by the two broad peaks at q_1 and q_2 which indicate a random dispersion of such bulky motives into the continuous aliphatic phase. A model for the packing based on WAXS and SPM experiments is sketched in Figure 2 where the lamellae distance,

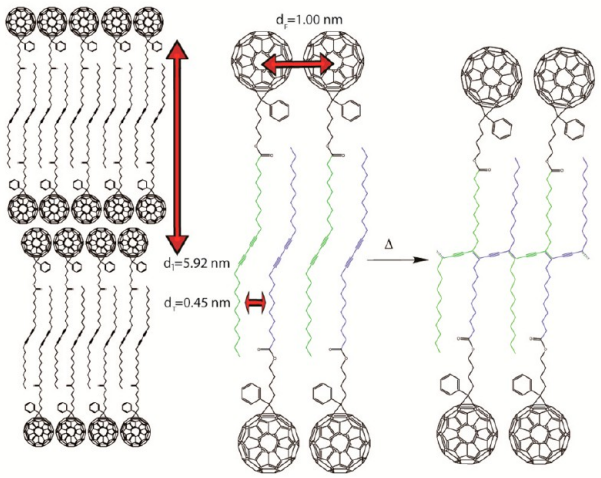

Figure 2. Schematics of the proposed self-assembly of C23 PCB-diyne and its solid-state polymerization reaction.

the fullerene−fullerene and the tail-to-tail distances are shown. A similar packing behavior in lamellae was observed by Chikamatsu and co-workers for a monoalkylated fullerene derivative.[38] We believe that the driving force for the lamellar arrangement is the immiscibility of the alkyl chains with the fullerenes on one hand and the tendency of the alkyl chains to crystallize on the other hand. The critical packing parameter (CPP) is commonly used to predict the packing ability of surfactant molecules in water from the curvature of the water−lipid interface. The CCP is obtained by comparing the volume of the lipid tail to the product of the cross-sectional area of the head and the length of the lipid chain.[39] For C23 PCB-diyne, a CPP of 0.13 was found. The conformation was calculated using the density functional theory (DFT) (see Figure S7, Supporting Information). From here one would expect a packing of the molecules into micelles.[40] We attribute the different observed packing behavior to three factors. Both the rigid diacetylene moiety in the middle of the alkyl chain, the use of an organic solvent which may change the effective chain excluded volume compared to a flexible alkyl chain in water,[41] and, last but not least, surface effects which may shift the observed conformation from micelles to lamellas. This observation is supported by a study by Nakanishi et al. where it was shown that fullerenes bearing long alkyl chains self-assembled into interdigitated bilayer structures independently on the CPP.[42]

Polymerization of C23 PCB-Diyne. Thermal polymerization was chosen among other possible polymerization methods to differentiate the topochemical reaction from the photopolymerization of the C_{60} alone.[43] Topochemical reactions occur over a wide temperature range with typical activation energies of 22 kcal mol^{-1}.[44] According to the WAXS data, annealing the films at 100 °C for 24 h sustained the micromorphology of the film; additionally, the film was left fully insoluble in the coating solvent. The above-discussed packing leads to a high degree of order in a film cast from CB that supports the solid-state polymerization mechanism. The theoretical polymer structure resulting from the topochemical reaction between multiple stacked diacetylenes is shown in Figure 2 for C23 PCB-diyne.[23] We sketch the transformation of a monomer-made lamella to an insoluble polymer-made lamella. Here the self-assembly of the C23 PCB-diyne provides the favored stacking of the diacetylene moieties.[20−22] The evolution of the morphology of the drop-casted films was explored by SPM in parallel to the WAXS experiment. According to the scattering data, no amorphous regions exist in the film; the SFM scans therefore show large polycrystalline domains embedded in a microcrystalline matrix (Figure 3a). These structures are stable against annealing at 100 °C (Figure 3b).

Annealing the film at 120 °C fully destroys the crystalline character of the film. This is confirmed by SFM scan (Figure 3c). The shape of large domains remains intact (Figures 3g,h), suggesting that the melt resulting from annealing does not flow. Interestingly, the polymerization reaction is also taking place in this film, rendering it insoluble in the casting solvent after 8 h of annealing. We must conclude that the observed tail-to-tail distance of 4.6 Å between the alkyl chains still allows for the topochemical polymerization.

For applications in optoelectronics, organic materials are typically deposited onto a substrate in a thin film. In the next section we discuss the behavior of PCB-diyne and PCB-diyne blend films spin-coated onto a substrate. Cross-linking was also observed for films of C23 PCB-diyne spin-coated from CB solution (see Figure S9, Supporting Information). With annealing time the PCB-diyne film partially dewetted and formed polycrystalline domains very similar to those obtained by drop-casting. We assume that the fast process of spin-coating does not allow the formation of an equilibrium morphology, and the annealing of the films induces a further chain rearrangement of the molecules until a configuration allowing for the topochemical reaction is adopted. The annealed polycrystalline films were insoluble in good solvents of the monomer such as CB, dichlorobenzene, dichloromethane, and chloroform, indicating a successful solid-state polymerization reaction. Similar to the drop-casted films, crystallization is not a necessary condition for polymerization. We recall here that

dx.doi.org/10.1021/ma401677v | Macromolecules 2014, 47, 721−728

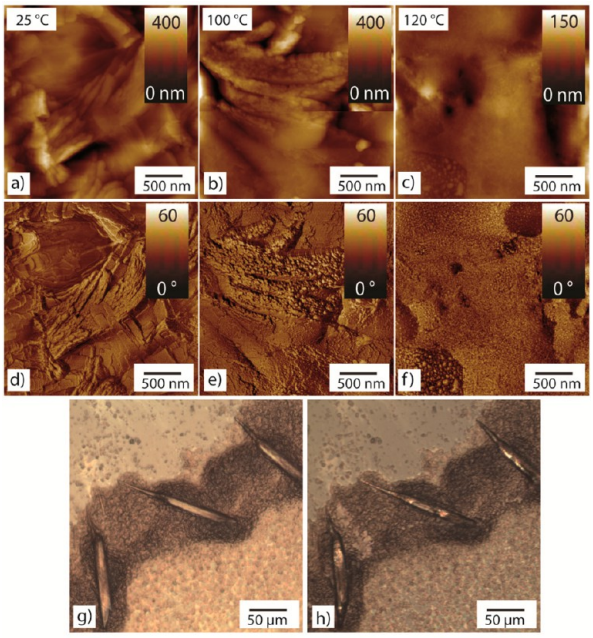

Figure 3. Stabilization of pure C23 PCB-diyne films: (a) SFM image of a drop-cast film before annealing; (b) after annealing at 100 °C; (c) after annealing at 120 °C; (d–f) corresponding phase images; (g) single crystals obtained by drop-casting a solution of 10 mg mL^{-1} C23 PCB-diyne in CB; (h) the same domains are insoluble after annealing 7 h at 120 °C, the film has been washed with CB.

only the local chain arrangement determines whether the reaction takes place.

FTIR spectroscopy, Raman spectroscopy, and DSC (Figures 4a,b) were used to monitor chemical changes upon annealing at

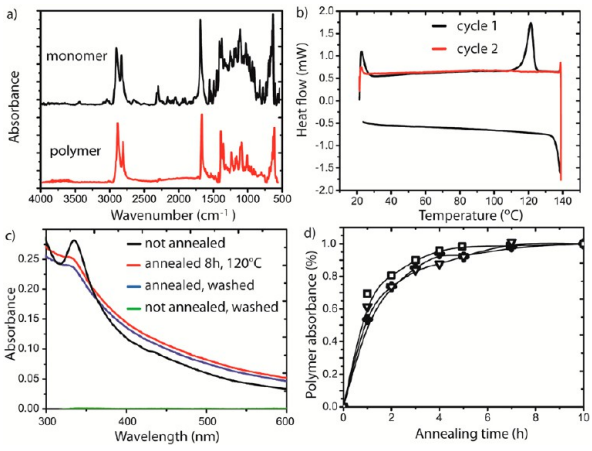

Figure 4. (a) FTIR spectra of as-coated C23 PCB-diyne film (top) and after annealing at 120 °C for 8 h (bottom). (b) DSC thermograms showing a thermoset behavior for C23 PCB-diyne. (c) Stabilization of pure C23 PCB-diyne films monitored with UV–vis spectroscopy (red: PCB-diyne film as-casted; black: after annealing; blue: annealed film after washing with CB; green: nonannealed film after washing with CB). (d) Kinetics of polymerization for C23 PCB-diyne films with thicknesses of 17 nm (square), 35 nm (triangle), and 100 nm (cross) upon annealing (120 °C). Films were washed with CB after indicated times, and the remaining absorbance at 330 nm was measured. All experiments conducted at 120 °C suggest that insolubility is not correlated to a high degree of polymerization. This renders chemical and structural analysis of the product challenging.[20]

120 °C. The characteristic FTIR absorption bands of the monomer at 2330, 2193, and 2077 cm^{-1}, which correspond to the stretching of the diacetylene moiety (C≡C–C≡C st), disappeared upon annealing. The alkene (C=C st) vibrations at ~1600 cm^{-1} was detected after annealing by Raman spectroscopy (see Figure S15, Supporting Information). These observations are in line with the reaction shown in Figure 2. In the DSC thermograms an endothermic melting point appeared at T_m = 122 °C during the first heating cycle. This observation is in agreement with the WAXS experiments. In the second heating cycle, however, the melting peak disappeared. The resulting thermoset does not recrystallize during cooling; neither does it melt in the second heating cycle due to a fixed conformation of the aliphatic chains. The polymerization reaction itself is predicted to be slightly exothermic.[45] We explain the absence of a signature for this process by the rearrangement of the alkyl chains over a broad range of temperatures prior to polymerization. We quantified the insolubility of the cross-linked films by immersing the samples in the solvent used for spin-coating and monitoring the absorbance changes by UV–vis spectroscopy. Figure 4c shows the absorbance spectra of as-cast films. The spectrum of the nonannealed film is almost identical to the spectrum of a pure PCBM film. The UV–vis spectrum of the annealed film differs from the nonannealed film; we observed a broadening of the characteristic absorption peak at 330 nm as well as a general increase in absorption at larger wavelengths. These changes reflect the crystallization and roughening of the film which was shown above. The polymerization of self-assembled diacetylene does not lead to new absorption bands in the UV–vis region due to polydiacetylenes of various length and conformation.[10] For a film annealed at 120 °C for 8 h or at 100 °C for 24 h, the absorption remained almost unaltered after solvent wash (Figure 4c and Figure S10), whereas the nonannealed film fully dissolved. Annealing of spin-coated films is also suitable to study the kinetics of PCB-diyne rearrangement and polymerization. In Figure 4d, we show the fraction of the film remaining on the substrate as determined by UV–vis as a function of annealing time. The stabilization time was almost the same for films of different thicknesses; full insolubility was in all cases reached after 5 h of annealing at 120 °C. Such a slow polymerization also supports the hypothesis that chain rearrangement has to occur prior to polymerization. The rate-limiting step is in this case the local ordering of molecules which allows consecutive rapid polymerization. TGA experiments were performed to exclude any degradation or weight loss in the range of annealing temperature (see Figure S11, Supporting Information).

We conducted a control experiment with a PCB-diyne with a much shorter alkyl-chain (C11). In that case, no insoluble phase was formed after annealing (see Figure S12). C11 PCB-diyne may not arrange into a structure that facilitates stacking of the diacetylene moieties necessary for polymerization. This finding is similar to recent results obtained for the polymerization of alkyldiacetylene in thin Langmuir–Blodgett films, where it was found that long, odd-numbered alkyl spacers yielded considerably better polymerization due to a better accommodation to the restrictive single crystal structure.[46–48] A second control experiment was carried out to demonstrate that the conjugated diacetylene units do not attack the fullerene moiety of PCB-diyne, leading to different cross-linked products. Blend films of PCBM and 10,12-tricosadiynoic acid were annealed for 8 h and were then washed with CB. PCBM could

dx.doi.org/10.1021/ma401677v | Macromolecules 2014, 47, 721–728

completely be removed with CB after annealing and the UV−vis spectrum of the washing solution coincides with the spectrum of the starting solution (see Figure S13). Thus, the major part of the fullerenes had not reacted during polymerization and remained intact.[49] This result is also supported by the Raman spectra shown in Figure S15.

C23 PCB-Diyne/CyC Blend Film Morphology. Fullerene derivatives are most widely used as model electron acceptors in blend organic photovoltaics. In this field, the ability to thermoset blend thin films may be crucial for stabilizing nanoscale phase-separated morphologies against aging or further processing. As an example to illustrate the general ability of PCB-diyne to stabilize blend morphologies, we study the blending of PCB-diyne and a cyanine dye, CyC. The cross-linking reaction also proceeds in the fullerene phase of a film of PCB-diyne blended with the cyanine dye CyC. The molecular structure of CyC is shown in Figure 5a. In Figure 5b, we show

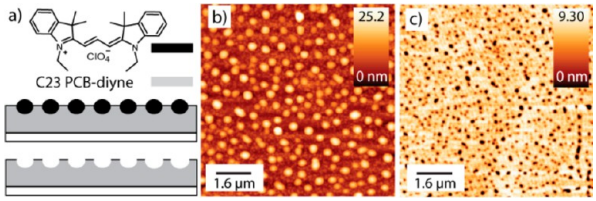

Figure 5. Blend morphology stabilization: (a) structure of the cyanine dye and sketch of vertically phase separated C23 PCB-diyne/CyC film; (b) SFM image of a 10:1 C23 PCB-diyne/CyC molar blend film coated at 500 rpm from CB; (c) SFM image of the insoluble mesostructured C23 PCB-diyne film after thermal polymerization and dissolution of CyC.

SFM scans of a C23-PCB-diyne/dye blend film with a molar ratio of 10:1. We found monodispersed droplets embedded in a matrix film. Selectively dissolving the dye leaves sinkholes in the matrix film as shown in the SFM scans in Figure 5c. The film morphology thus comprises droplets of CyC in a matrix of PCB-diyne. A sketch of the film morphology is shown in Figure 5a. We can explain the morphologies obtained from the phase separation of the C23 PCB-diyne/CyC system by liquid−liquid dewetting similarly to the PCBM/CyC blend system which we investigated earlier.[30] In the case of PCBM, a transient bilayer forms with PCBM in contact with air and CyC in contact with the substrate. Because of the higher surface energy of C23 PCB-diyne compared to PCBM (60 and 18 mN m^{-1}, respectively), the order of the initial transient bilayer is reversed, with CyC (34.3 mN m^{-1}) and C23 PCB-diyne now forming wetting layers at the air and substrate interface, respectively. For low dye fractions, the top dye layer dewets from the PCB-diyne layer, forming the pattern of monodispersed dye droplets on top of a PCB-diyne matrix film.

C23 PCB-diyne in blend films can also be thermally polymerized. After washing in the casting solvent, this method conserves the same morphology as dissolving the dye in a selective solvent without polymerization (Figure 5c). This experiment and the UV−vis spectra of annealed and non-annealed films shown in Figure S12 prove that the C23 PCB-diyne phase can be selectively rendered insoluble in blends. Differently from the pure C23 PCB-diyne films, no large polycrystalline domains formed during annealing as shown in Figure 5c. This indicates that the dispersed solid CyC droplet phase seems to hinder the growth of large polycrystals. The polymerization still proceeds in blends. The morphology shown in Figure 5 is one example of PCB-diyne morphologies which can be stabilized and forms the basis of fullerene scaffolds. Depending on mixing ratios and film thicknesses, a large variety of PCB-diyne morphologies can be manufactured (see Figure S14).

C23 PCB-Diyne/CyC Blend Films on Patterned Substrates. Figure 6a shows SFM scans of the morphology

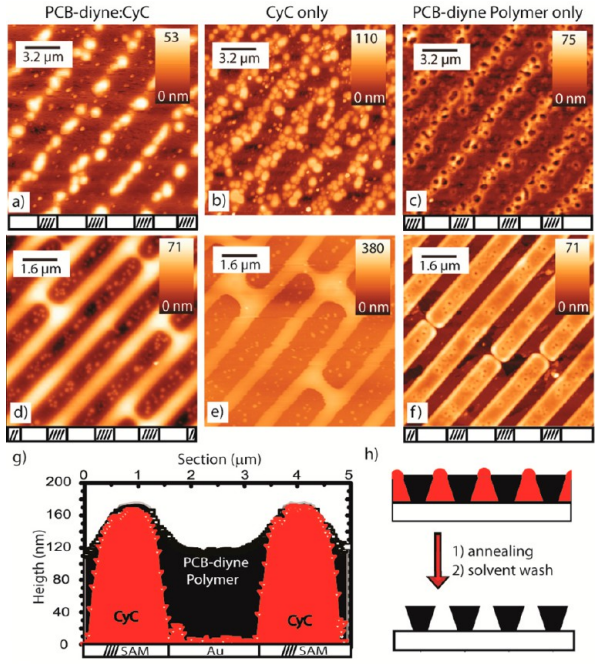

Figure 6. 1D template formation and stabilization: (a) SFM image of a C23 PCB-diyne/CyC blend film on a SAM stripe pattern as indicated below the figure (1:1 molar blend 1 wt % in CB, spin-coated at 500 rpm); (b) C23 PCB-diyne selectively removed with hexane; (c) CyC selectively removed with CB after thermal polymerization of PCB-diyne; (d) increasing the dye volume fraction in the film leads to an optimized pattern transfer (1:2 C23 PCB-diyne/CyC molar blend 1 wt % in CB, 500 rpm); (e) C23 PCB-diyne selectively removed with hexane; (f) CyC selectively removed with CB after thermal polymerization of C23 PCB-diyne; (g) experimental cross section of the patterned morphology; (h) sketch of the process that leads to an undercut structure.

of a C23 PCB-diyne/CyC blend film coated from a solution with a 1:1 molar ratio onto a SAM stripe pattern. Figures 6b and 6c show corresponding scans after PCB-diyne and CyC has been selectively dissolved, respectively. We find cyanine droplets embedded in a PCB-diyne matrix, whereby the cyanine only forms a phase above the SAM stripes.

Increasing the volume fraction of dye in the film leads to a situation where the dye fully covers the SAM stripes (Figures 6d−f). This structure forms because CyC wetting droplets are pinned to the SAM−gold interface. We achieved an almost perfect transfer of the chemical substrate pattern into a phase pattern. The corresponding imprinted and structured PCB-diyne phase could also be thermally stabilized against solvents (Figure 6f). With this contact-line pinning method we were able to fabricate undercut structures (Figures 6g,h) which are challenging to achieve with top-down methods such as photolithography. The angle of the undercut structure depends on the dye volume fraction.[35] This is one very specific example on how we can design photonic structures with the PCB-diyne/

dx.doi.org/10.1021/ma401677v | Macromolecules 2014, 47, 721−728

dye blend system. Films with topographical or compositional pattern scatter ligh coherently.[50] The materials and processes can be utilized more generally for photonic applications: the self-assembled fullerene itselves can possess useful optical properties; here we specifically think of materials with high dielectric constants.[51] Polymer templates are frequently used as base material for photonic materials[52] and can act as matrix for optically active materials.[53]

CONCLUSION

We synthesized a fullerene derivative which self-assembles into lamellar structures. The self-assembly in these nanostructures leads to an arrangement of diacetylene moieties such that a topochemical solid-state polymerization takes place upon annealing at 100 °C, stabilizing the self-assembled morphology and rendering the film insoluble in common solvents. The associated chemistry is more straightforward than the chemistry following a pathway based on the common belief that effective cross-linking requires at least two diyne moieties.[4] Annealing the sample at 120 °C above the order−disorder transition of the material also leads to a cross-linked insoluble film that is now mainly amorphous. That is surprising as a certain chain arrangement is prerequisite for the solid-state polymerization. We conclude that to reach insolubility only a low number of ordered cross-linking sites are necessary. The cross-linking reaction also proceeds in spin-coated films but is accompanied by large scale dewetting and crystallization. Most interestingly, the reaction occurs in the C23 PCB-diyne phase of blend films, opening a way to fabricate complex 3D insoluble objects. In this case the large-scale crystallization is hindered by the presence of dispersed dye domains. Selectively removing the dye after polymerization of the C23 PCB-diyne leaves structured fullerene scaffolds. The C23 PCB-diyne templates show mesoporous structures in the submicrometer range; we are currently investigating the feasibility of this process for manufacturing nanoporous structures.

ASSOCIATED CONTENT

Supporting Information

Mass spectrometry (MS) of C23 PCB-diyne, NMR of intermediates and products, UV−vis spectra of C23 and C11 PCB-diyne/CyC films, UV−vis spectra of PCBM/10,12-tricosadiynoic acid blends, TGA of C23 PCB-diyne, optimal molecular conformation calculated by DFT, SFM of bulk and blend spin-coated morphologies, Raman spectroscopy of pristine and annealed C23 PCB-diyne. This material is available free of charge via the Internet at http://pubs.acs.org.

AUTHOR INFORMATION

Corresponding Author

*E-mail jakob.heier@empa.ch (J.H.).

Notes

The authors declare no competing financial interest.

ACKNOWLEDGMENTS

We thank Beatrice Fischer (Empa) for DSC and TGA measurements, Ylenia Maniglio (Empa) for help in the synthesis, M. Nagel (Empa) for helpful discussions, and A. Gerecke (Empa) for MS measurements. We thank T. Geiger (Empa) for the molecular conformation simulations. This work was supported by the Swiss Competence Center for Energy and Mobility, CCEM-CH, Dursol project, and by the Swiss National Science Foundation (SNF) under grant number 200021_132502.

REFERENCES

(1) Makarova, T. L. In *Semiconductors*; American Institute of Physics: Melville, NY, 2001; Vol. 35, pp 243−278.
(2) Dresselhaus, M. S.; Dresselhaus, G. *Annu. Rev. Mater. Sci.* **1995**, *25*, 487−523.
(3) Prassides, K.; Keshavarz, M.; Beer, E.; Bellavia, C.; Gonzalez, R.; Murata, Y.; Wudl, F.; Cheetham, A. K.; Zhang, J. P. *Chem. Mater.* **1996**, *8*, 2405−2408.
(4) Sawamura, M.; Kawai, K.; Matsuo, Y.; Kanie, K.; Kato, T.; Nakamura, E. *Nature* **2002**, *419*, 702−705.
(5) Georgakilas, V.; Pellarini, F.; Prato, M.; Guldi, D. M.; Melle-Franco, M.; Zerbetto, F. *Proc. Natl. Acad. Sci. U. S. A.* **2002**, *99*, 5075−5080.
(6) Babu, S. S.; Mohwald, H.; Nakanishi, T. *Chem. Soc. Rev.* **2010**, *39*, 4021−4035.
(7) Cassell, A. M.; Asplund, C. L.; Tour, J. M. *Angew. Chem.,Int. Ed.* **1999**, *38*, 2403−2405.
(8) Zhou, S. Q.; Burger, C.; Chu, B.; Sawamura, M.; Nagahama, N.; Toganoh, M.; Hackler, U. E.; Isobe, H.; Nakamura, E. *Science* **2001**, *291*, 1944−1947.
(9) Nakanishi, T. *Chem. Commun.* **2010**, *46*, 3425−3436.
(10) Wang, J. B.; Shen, Y. F.; Kessel, S.; Fernandes, P.; Yoshida, K.; Yagai, S.; Kurth, D. C.; Mohwald, H.; Nakanishi, T. *Angew. Chem., Int. Ed.* **2009**, *48*, 2166−2170.
(11) Nakanishi, T.; Schmitt, W.; Michinobu, T.; Kurth, D. G.; Ariga, K. *Chem. Commun.* **2005**, *48*, 5982−5984.
(12) Nakanishi, T.; Miyashita, N.; Michinobu, T.; Wakayama, Y.; Tsuruoka, T.; Ariga, K.; Kurth, D. G. *J. Am. Chem. Soc.* **2006**, *128*, 6328−6329.
(13) Drees, M.; Hoppe, H.; Winder, C.; Neugebauer, H.; Sariciftci, N. S.; Schwinger, W.; Schaffler, F.; Topf, C.; Scharber, M. C.; Zhu, Z. G.; Gaudiana, R. *J. Mater. Chem.* **2005**, *15*, 5158−5163.
(14) Cheng, Y. J.; Hsieh, C. H.; Li, P. J.; Hsu, C. S. *Adv. Funct. Mater.* **2011**, *21*, 1723−1732.
(15) Cheng, Y. J.; Cao, F. Y.; Lin, W. C.; Chen, C. H.; Hsieh, C. H. *Chem. Mater.* **2011**, *23*, 1512−1518.
(16) Markov, D. E.; Amsterdam, E.; Blom, P. W. M.; Sieval, A. B.; Hummelen, J. C. *J. Phys. Chem. A* **2005**, *109*, 5266−5274.
(17) Nierengarten, J. F.; Setayesh, S. *New J. Chem.* **2006**, *30*, 313−316.
(18) Wegner, G. *Z. Naturforsch., Part B* **1969**, *B24*, 824.
(19) Schmidt, G. M. T. In *Solid State Photochemistry*; Verlag Chemie: Weinheim, 1976.
(20) Enkelmann, V. In *Polydiacetylenes*; Cantow, H.-J., Ed.; Springer: Berlin, 1984; Vol. *63*, p 91.
(21) Baughman, R. H. *J. Polym. Sci., Part B: Polym. Phys.* **1974**, *12*, 1511−1535.
(22) Enkelmann, V. *Colloid Polym. Sci.* **1978**, *256*, 893−903.
(23) Khandelwal, P. K.; Talwar, S. S. *J. Polym. Sci., Part A: Polym. Chem.* **1983**, *21*, 3073−3082.
(24) Stein, A. *Adv. Mater.* **2003**, *15*, 763−775.
(25) Blom, P. W. M.; Mihailetchi, V. D.; Koster, L. J. A.; Markov, D. E. *Adv. Mater.* **2007**, *19*, 1551−1566.
(26) Hoppe, H.; Sariciftci, N. S. *J. Mater. Chem.* **2006**, *16*, 45−61.
(27) Sary, N.; Richard, F.; Brochon, C.; Leclerc, N.; Leveque, P.; Audinot, J. N.; Berson, S.; Heiser, T.; Hadziioannou, G.; Mezzenga, R. *Adv. Mater.* **2010**, *22*, 763−768.
(28) Dang, M. T.; Hirsch, L.; Wantz, G.; Wuest, J. D. *Chem. Rev.* **2013**, *113*, 3734−3765.
(29) Mishra, A.; Bauerle, P. *Angew. Chem., Int. Ed.* **2012**, *51*, 2020−2067.
(30) Heier, J.; Groenewold, J.; Huber, S.; Nuesch, F.; Hany, R. *Langmuir* **2008**, *24*, 7316−7322.
(31) Kumar, A.; Whitesides, G. M. *Appl. Phys. Lett.* **1993**, *63*, 2002−2004.

(32) Love, J. C.; Estroff, L. A.; Kriebel, J. K.; Nuzzo, R. G.; Whitesides, G. M. *Chem. Rev.* **2005**, *105*, 1103−1169.
(33) Xue, L. J.; Han, Y. C. *Prog. Polym. Sci.* **2011**, *36*, 269−293.
(34) Boltau, M.; Walheim, S.; Mlynek, J.; Krausch, G.; Steiner, U. *Nature* **1998**, *391*, 877−879.
(35) Tisserant, J. N.; Hany, R.; Partel, S.; Bona, G. L.; Mezzenga, R.; Heier, J. *Soft Matter* **2012**, *8*, 5804−5810.
(36) Ernst, L. A.; Gupta, R. K.; Mujumdar, R. B.; Waggoner, A. S. *Cytometry* **1989**, *10*, 3−10.
(37) Horcas, I.; Fernández, R.; Gómez-Rodríguez, J. M.; Colchero, J.; Gómez-Herrero, J.; Baro, A. M. *Rev. Sci. Instrum.* **2007**, *78*, 013705.
(38) Chikamatsu, M.; Nagamatsu, S.; Yoshida, Y.; Saito, K.; Yase, K.; Kikuchi, K. *Appl. Phys. Lett.* **2005**, *87*, 203504.
(39) Israelachvili, J. N. In *Intermolecular and Surface Forces*, 2nd ed.; Academic: New York, 1991.
(40) Mezzenga, R.; Schurtenberger, P.; Burbidge, A.; Michel, M. *Nat. Mater.* **2005**, *4*, 729−740.
(41) Birshtein, T. M.; Skvortsov, A. M.; Sariban, A. A. *Macromolecules* **1976**, *9*, 892−895.
(42) Nakanishi, T.; Shen, Y. F.; Wang, J. B.; Li, H.; Fernandes, P.; Yoshida, K.; Yagai, S.; Takeuchi, M.; Ariga, K.; Kurth, D. G.; Möhwald, H. *J. Mater. Chem.* **2010**, *20*, 1253−1260.
(43) Rao, A. M.; Zhou, P.; Wang, K. A.; Hager, G. T.; Holden, J. M.; Wang, Y.; Lee, W. T.; Bi, X. X.; Eklund, P. C.; Cornett, D. S.; Duncan, M. A.; Amster, I. J. *Science* **1993**, *259*, 955−957.
(44) Chance, R. C.; Patel, G. N. *J. Polym. Sci., Polym. Phys. Ed.* **1978**, *16*, 859−881.
(45) Rubner, M. F. *Macromolecules* **1986**, *19*, 2114−2128.
(46) Menzel, H.; Mowery, M. D.; Cai, M.; Evans, C. E. *J. Phys. Chem. B* **1998**, *102*, 9550−9556.
(47) Menzel, H.; Mowery, M. D.; Cai, M.; Evans, C. E. *Macromolecules* **1999**, *32*, 4343−4350.
(48) Menzel, H.; Horstmann, S.; Mowery, M. D.; Cai, M.; Evans, C. E. *Polymer* **2000**, *41*, 8113−8119.
(49) Xu, S. L.; Kang, S. Z.; Gan, L. B.; Zhang, L.; Wang, C.; Wan, L. J.; Bai, C. L. *Appl. Phys. A: Mater. Sci. Process.* **2003**, *77*, 757−760.
(50) Xia, Y. N.; Gates, B.; Li, Z. Y. *Adv. Mater.* **2001**, *13*, 409−413.
(51) Koster, L. J. A.; Shaheen, S. E.; Hummelen, J. C. *Adv. Energy Mater.* **2012**, *2*, 1246−1253.
(52) Braun, P. V.; Rinne, S. A.; Garcia-Santamaria, F. *Adv. Mater.* **2006**, *18*, 2665−2678.
(53) Lindsay, G. A.; Ashley, P. R.; Davis, M. C.; Guenthner, A. J.; Sanghadasa, M.; Wright, M. E. *Mater. Sci. Eng., B* **2006**, *132*, 8−15.